

See discussions, stats, and author profiles for this publication at: <https://www.researchgate.net/publication/253328299>

# Direct laser initiation and improved thermal stability of nitrocellulose/graphene oxide nanocomposites

Article in *Applied Physics Letters* · April 2013

DOI: 10.1063/1.4801846

CITATIONS

60

READS

473

7 authors, including:



**Xin Zhang**

Pacific Northwest National Laboratory

112 PUBLICATIONS 2,641 CITATIONS

[SEE PROFILE](#)



**Walid Hikal**

Texas Tech University

29 PUBLICATIONS 411 CITATIONS

[SEE PROFILE](#)



**Yue Zhang**

Georgia Southern University

42 PUBLICATIONS 1,570 CITATIONS

[SEE PROFILE](#)



**Sanjoy Bhattacharia**

Texas Tech University

28 PUBLICATIONS 476 CITATIONS

[SEE PROFILE](#)

Some of the authors of this publication are also working on these related projects:



Chemistry of the aluminate ion [View project](#)



Nanodiamond arrays [View project](#)

## Direct laser initiation and improved thermal stability of nitrocellulose/graphene oxide nanocomposites

Xin Zhang, Walid M. Hikal, Yue Zhang, Sanjoy K. Bhattacharia, Li Li et al.

Citation: *Appl. Phys. Lett.* **102**, 141905 (2013); doi: 10.1063/1.4801846

View online: <http://dx.doi.org/10.1063/1.4801846>

View Table of Contents: <http://apl.aip.org/resource/1/APPLAB/v102/i14>

Published by the [American Institute of Physics](http://www.aip.org).

---

### Additional information on *Appl. Phys. Lett.*

Journal Homepage: <http://apl.aip.org/>

Journal Information: [http://apl.aip.org/about/about\\_the\\_journal](http://apl.aip.org/about/about_the_journal)

Top downloads: [http://apl.aip.org/features/most\\_downloaded](http://apl.aip.org/features/most_downloaded)

Information for Authors: <http://apl.aip.org/authors>

## ADVERTISEMENT



**AIP** | Applied Physics Letters

Accepting Submissions in  
Biophysics and Bio-Inspired Systems

*Submit Today*

**AIP**  
Publishing

## Direct laser initiation and improved thermal stability of nitrocellulose/graphene oxide nanocomposites

Xin Zhang,<sup>1</sup> Walid M. Hikal,<sup>1,2,a)</sup> Yue Zhang,<sup>3</sup> Sanjoy K. Bhattacharia,<sup>1</sup> Li Li,<sup>3</sup> Siddharth Panditrao,<sup>1</sup> Shiren Wang,<sup>3</sup> and Brandon L. Weeks<sup>1,a)</sup>

<sup>1</sup>Department of Chemical Engineering, Texas Tech University, Lubbock, Texas 79409, USA

<sup>2</sup>Department of Physics, Faculty of Science, Assiut University, Assiut 71516, Egypt

<sup>3</sup>Department of Industrial Engineering, Texas Tech University, Lubbock, Texas 79409, USA

(Received 16 January 2013; accepted 1 April 2013; published online 9 April 2013)

We report on the enhancement and possible control of both laser ignition and burn rates of Nitrocellulose (NC) microfilms when doped with graphene oxide (GO). A Nd:YAG (1064 nm, 20 ns) laser is used to ignite GO-doped NC films at low temperatures. The effect of GO on the doping concentration of the activation energies of laser ignition and thermal stability of the NC films is studied. The activation energy of laser ignition decreases with increasing GO/NC weight ratio and attains a constant value with higher concentrations. This behavior is accompanied by an increase in the thermal stability. © 2013 AIP Publishing LLC. [<http://dx.doi.org/10.1063/1.4801846>]

Nitrocellulose (NC) is an important industrial polymer with wide-ranging applications in coatings, propellants, filtration, and membranes for the isolation of proteins, RNA, and DNA.<sup>1</sup> It is also a typical energetic material fill, and remains a leading ingredient of gunpowder and solid rocket propellants formulations.<sup>2–7</sup> Developing efficient and low cost methods for manipulating multidimensional micro/nanoscale NC and its composites, and enhancing their ignition and combustion behaviors, is very important for improving high speed propulsion systems. The ability to control the decomposition pathways for such materials is also of interest since it leads to optimal performance and controlled energy release.

Graphene oxide (GO) is one of the most important functional graphene materials and is often used to synthesize various graphene supported nanocomposites.<sup>8–10</sup> GO contains abundant oxygen-containing groups on the basal planes and edges which gives superior dispersion in various solvents including water as compared to pure graphene. GO has also been used to aid in the formation of nano-/micro-scale particles of organic/inorganic materials on its surface through hydrogen bonding,  $\pi$ - $\pi$  stacking, or electrostatic interactions.<sup>11–13</sup> For example, in polymer-based nanocomposites, GO has been shown to have excellent mechanical reinforcement<sup>14–18</sup> and can increase glass transition temperature ( $T_g$ ) of polymers.<sup>14,19,20</sup> The enhanced properties are attributed to hydrogen-bonding interactions between polymers and GO or/and nanoconfinement between two or more GO layers.<sup>7–20</sup>

Here, we report on the simple fabrication of highly porous microfilms of nitrocellulose by doping NC with graphene oxide from 0.05% to 3% weight ratios. The direct IR laser ignition and burn rate of the microfilms, as well as their thermal stability against decomposition, are included.

Pristine graphite flakes, sized at 45  $\mu\text{m}$ , were provided by Asbury Carbons (Asbury, NJ). NC (4%–8% in ethanol/diethyl ether, 11.8–12.2 wt. % nitrogen) was purchased from Sigma-

Aldrich, Inc. The GO was prepared by a modified Brodie's method.<sup>21</sup> Pure and GO-doped NC films are obtained through mixing pure NC-acetone solution and various weight ratios of GO water solution. The mixture is added drop-wise to a substrate, allowed to evaporate at ambient temperature, and then dried at 70 °C in a vacuum oven. The thickness of these films can be controlled by the amount of solution added to the substrate. Scanning electron microscopy (SEM) images were collected by Hitachi S4300 scanning electron microscope. The pure NC and GO-NC films were sputter coated a thin layer of gold prior to imaging to ensure good conductivity and imaging. Atomic force microscopy (AFM) images were obtained with a Nanoscope IIIa multimode AFM (Veeco, Santa Barbara, CA) operating in tapping mode. All Differential Scanning Calorimeter (DSC) measurements (TA Instruments, Model Q20) were collected from 40 to 400 °C in crimped aluminum pans at heating rates of 2, 5, 7.5, and 10 °C/min. Burn rates were measured in air using a digital high-speed infrared camera (Phantom v710) initiated by a CO<sub>2</sub> laser (Firestar f-series, 400 W, 10 200–10 800 nm) at room temperature. To determine the activation energy for optical initiation, the laser ignition a pulsed Tempest 10 (Portland, OR) Nd:YAG laser (1064 nm) was used with a 10 mm focal length lens. Data were collected from 100 to 180 °C and the energy density (fluence) was varied by changing the distance between the lens and the film.

Fig. 1 represents the different morphologies of the Pure NC and GO-doped NC films as observed by SEM and AFM. As shown in Fig. 1(a), the pure NC films are continuous, smooth, and have no observable microstructure. After introducing GO to the NC films, the morphology of the NC films varies significantly. The NC film's surfaces become rough when doped with just 0.1% GO (Fig. 1(b)). Further increase in the concentration of GO leads to highly porous networks after doping with 0.5% or more GO (Figs. 1(c)–1(e)). In comparison with the 0.5% GO-doped NC, the 1% GO-doped sample shows larger pores with diameters from 0.5  $\mu\text{m}$  to 3  $\mu\text{m}$ , which is also confirmed by atomic force microscopy studies, as shown in Fig. 1(g). Uniform films could not be fabricated at concentrations above 3% GO. Micrograph of

<sup>a)</sup>Authors to whom correspondence should be addressed. Electronic addresses: Walid.hikal@ttu.edu and brandon.weeks@ttu.edu

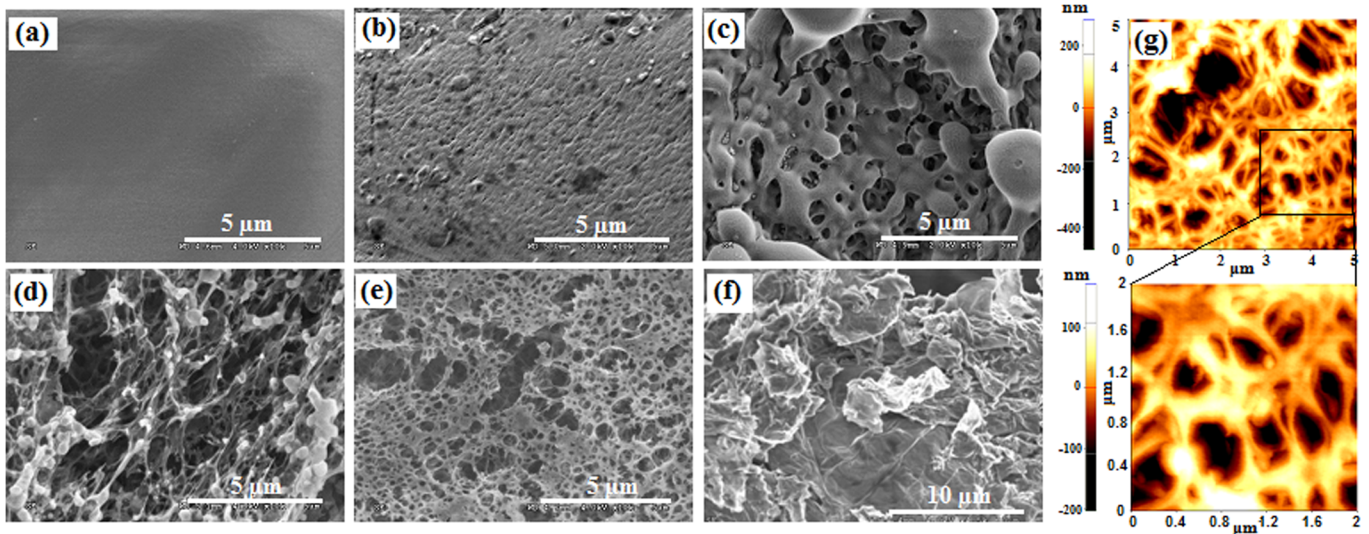


FIG. 1. SEM and AFM images of pure and GO doped NC films. SEM image of (a) pure NC film, (b) 0.1%, (c) 0.5%, (d) 1%, and (e) 2% GO doped NC film; (f) as-produced GO; (g) AFM images of 1% GO doped NC film.

the as-produced GO is shown in Figure 1(f) for comparison. The size of GO flakes ranges from 0.5  $\mu\text{m}$  to 6  $\mu\text{m}$ .

Pure NC films cannot be ignited with the highest fluence used in this study ( $\sim 20 \text{ J/cm}^2$ ). This is most likely due to the absence of significant optical absorbance band for NC in the IR region of our laser. However, with the addition of GO, direct laser ignition is possible. The activation energies of laser ignition of the microfilms are calculated as follows.

For the laser ignition of the GO-NC films, it was assumed that the ignition probability (the number of samples exploded out of ten samples initiated) is described by the normal distribution function<sup>21</sup>

$$P = \Phi\left(\frac{W - \bar{W}}{\sigma}\right), \quad (1)$$

where  $W$  is the laser radiation fluence,  $\bar{W}$  is its mean value (ensuring a 50% initiation probability),  $\sigma$  is the mean-square deviation, and  $\Phi$  is the probability integral given by

$$\Phi(U) = \frac{1}{\sqrt{2\pi}} \int_{-\infty}^U e^{-\frac{t^2}{2}} dt. \quad (2)$$

The data obtained for each doping concentration were analyzed in terms of temperature-dependent Arrhenius behavior in the form:

$$W_{0.5} = A \exp\left(-\frac{E_a}{k_B T}\right), \quad (3)$$

where  $A$  is the pre-exponential factor,  $E_a$  is the activation energy of ignition,  $k_B$  is the Boltzmann constant, and  $T$  is the absolute temperature. This equation can be written in the form:

$$\text{Ln}(W_{0.5}) = \text{Ln } A - \frac{E_a}{k_B} \frac{1}{T}. \quad (4)$$

Thus, a plot of the logarithm of the 50% ignition probability versus the inverse of temperature results in a straight line from which the activation energy can be determined.<sup>22</sup>

Fig. 2(a) shows plots of the logarithm of the fluence corresponding to 50% probability of successful ignition of the films with different doping concentrations versus the inverse of the absolute temperature. The results show good agreement with the Arrhenius behavior where straight lines are

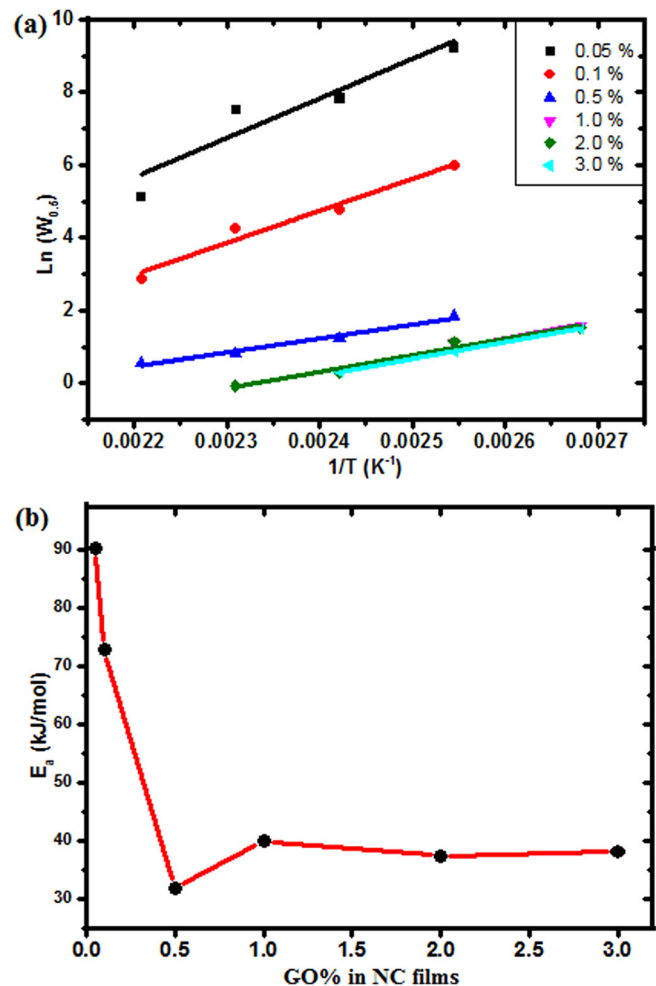


FIG. 2. (a) Arrhenius plots of the GO doped NC films; (b) comparison of the activation energy with GO concentration.



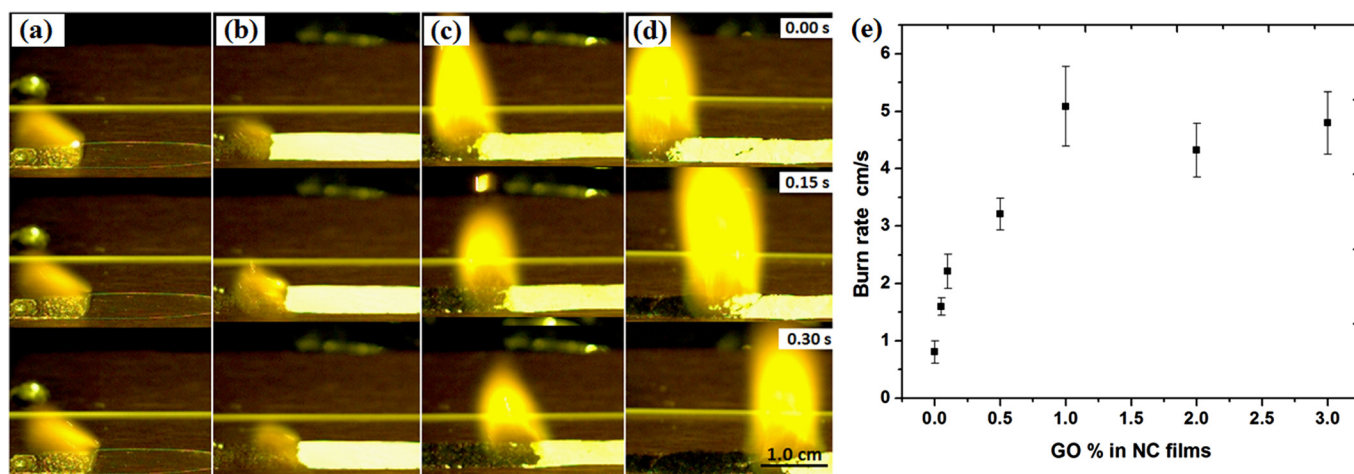


FIG. 3. High speed images of combustion process of pure NC films and GO-NC films in ambient conditions: (a) Pure NC film; (b) 0.05% GO-NC film; (c) 0.5% GO-NC film; (d) 1% GO-NC film. (e) Comparison of the burn rates of pure NC films and GO-NC films.

obtained for all films. These plots were used to calculate the activation energy for laser ignitions of all concentrations used in this study according to Arrhenius equation as shown in Fig. 2(b). The activation energy of ignition decreases with increasing the GO concentration and reaches a constant value at 0.5% and higher wt ratios. Since the temperature dependence of  $W_{0.5}$  can be described by an Arrhenius expression indicates that a thermally activated process may contribute to the initiation mechanism.

We suggest this significant enhancement in laser ignition with the addition of GO to NC is a result of the fact that GO is a good infrared light absorber.<sup>22,23</sup> The most likely method of initiation is the conversion of optical energy to heat which initiates the reaction. GO has been shown to generate local heat under IR laser irradiation due to the broad absorption band.<sup>23,24</sup> The initiation threshold can also be reduced by the increased surface area of the composite films. Previous studies have shown that high surface area NC is less thermally stable than bulk NC which should lead to easier initiation.<sup>5</sup>

The reaction of pure NC and GO-doped NC films is a deflagration rather than a detonation. Therefore, the burn

rates can be easily observed using high speed imaging as shown in Fig. 3. The addition of GO results in a significant enhancement in burn rate compared to that of the pure NC films. The increase in burn rate is roughly linearly proportional to the GO additive concentration from 0.05% to 1.0% where it reaches a maximum value that is  $\sim 500\%$  larger than that of the pure NC films. This significant enhancement in burn rates with the addition of GO cannot be solely attributed to the presence of GO in the NC films since there is a significant increase in surface area of NC films, which has also been shown to increase the burn rate.

Thermal analysis was conducted using differential scanning calorimetry. Decomposition kinetics of the pure NC and GO-doped NC films are obtained by using Ozawa model,<sup>25–27</sup> which is presented as follows:

$$\log \beta = -0.4567 \left( \frac{E_a}{RT_m} \right) - 2.315 + \log \frac{A_T E_a}{R} - \log g(\alpha), \quad (5)$$

where  $\beta$  is the heating rate,  $E_a$  is the activation energy,  $R$  is the gas constant,  $T_m$  is the peak temperature of the DSC

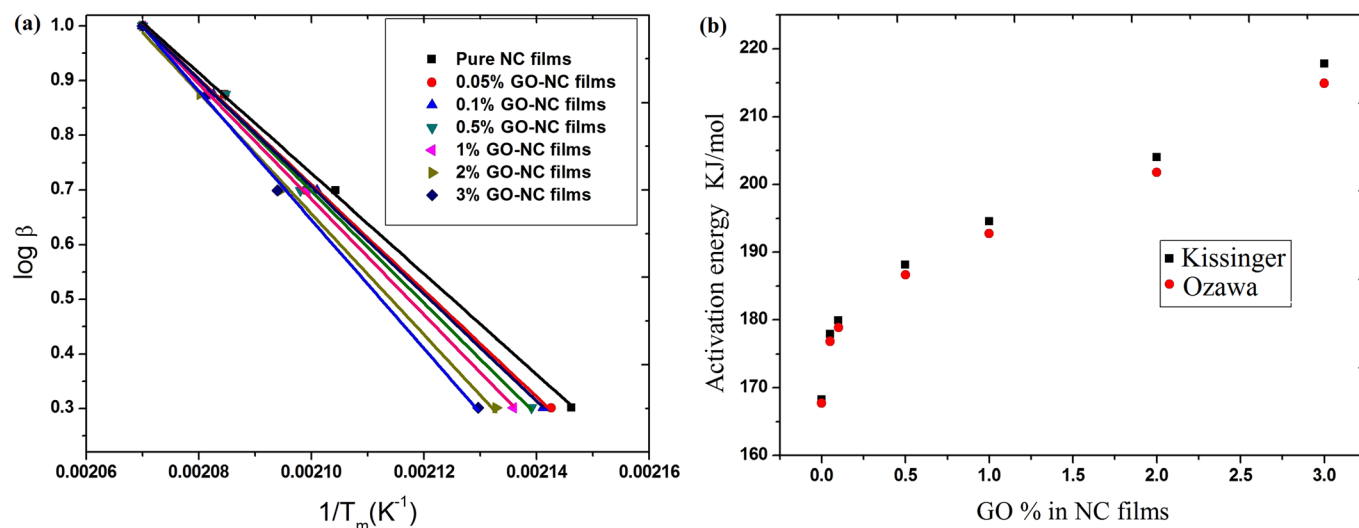


FIG. 4. (a) Plot of  $\ln(\beta)$  versus the reciprocal of the peak temperature  $1/T_m$  for pure NC and GO-NC films, note that temperature is normalized for all samples to the pure NC for comparison; (b) plot of activation energy of pure NC and GO-NC films versus GO concentration for both the Ozawa and Kissinger models.

curve,  $A_T$  is the frequency factor for thermal decomposition,  $\alpha$  is the extent of reaction, and  $g(\alpha)$  is a function of extent of reaction. DSC data were fitted in Eq. (5) and presented in Figure 4(a). For comparison of the slope, the initial onset value for each composite is normalized to the pure NC. This normalization does not affect the activation energy and is performed to aid in the comparison of the data. The plots of the logarithm of heating rate ( $\beta$ ) as a function of the reciprocal of the peak temperature are linear with  $R^2$  value greater than 0.99. Activation energies for all the samples are obtained from the slopes of the fitted lines. Linearity of the plots of all the GO doped and pure samples indicates that the reaction order of pure and GO doped nitrocellulose was similar. The symmetry of the decomposition peaks of the DSC curves of the films did not change as a function of the percentage decomposed indicating that addition of GO did not change the decomposition mechanism of nitrocellulose.<sup>27</sup>

To verify the accuracy of the values of the activation energy of decomposition, kinetic analysis is also conducted by using the Kissinger model.<sup>28</sup> In this model, the activation energy is obtained from the slope of the plot of  $-\ln \frac{\beta}{T^2}$  vs  $\frac{1}{T}$  multiplied by the gas constant. Activation energy obtained from both methods is presented in Fig. 4(b). Both methods produced similar values of activation energies of decomposition indicating a consistency in the experimental results.

As shown in Fig. 4(b), the activation energy of decomposition of NC increases significantly with the initial addition of GO and is essentially linear with increasing concentration of GO. The enhanced thermal stability of GO doped NC is in agreement with the theoretically predicted increase for 1:1 weight ratio of different explosives molecules, in activation energy of decomposition.<sup>29</sup>

In summary, the laser ignition and combustion behaviors of the GO doped NC films have been studied by using a Nd:YAG laser and digital high-speed imaging. The results showed that the laser ignition and burning rates of NC films were obviously improved when doped with 0.5% or more GO. The thermal analysis results also showed the GO doped NC films have higher activation energies of decomposition than pure NC films indicating a higher thermal stability.

The authors are exceedingly grateful for support received from NSF CAREER (CBET-0644832) and ONR (N00014-11-1-0424). Dr. Wang is also grateful to the

funding support from National Science Foundation (CMMI No. 1129914)

- <sup>1</sup>I. Wong and T. M. Lohman, *Proc. Natl. Acad. Sci. U.S.A.* **90**, 5428 (1993).
- <sup>2</sup>A. Chin, D. S. Ellison, S. K. Poehlein, and M. K. Ahn, *Propellants, Explos., Pyrotech.* **32**, 117 (2007).
- <sup>3</sup>C. P. Lin, Y. M. Chang, J. P. Gupta, and C. M. Shu, *Process Saf. Environ. Prot.* **88**, 413 (2010).
- <sup>4</sup>S. M. Pourmortazavi, S. G. Hosseini, M. Rahimi-Nasrabadi, S. S. Hajimirsadeghi, and H. Momenian, *J. Hazard. Mater.* **162**, 1141 (2009).
- <sup>5</sup>M. R. Sovizi, S. S. Hajimirsadeghi, and B. Naderizadeh, *J. Hazard. Mater.* **168**, 1134 (2009).
- <sup>6</sup>G. R. Peterson, K. A. Cychosz, M. Thommes, and L. J. Hope-Weeks, *Chem. Commun.* **48**, 11754 (2012).
- <sup>7</sup>W. Wei, X. Jiang, L. Lu, X. Yang, and X. Wang, *J. Hazard. Mater.* **168**, 838 (2009).
- <sup>8</sup>Y. Zhu, S. Murali, W. Cai, X. Li, J. W. Suk, J. R. Potts, and R. S. Ruoff, *Adv. Mater.* **22**, 3906 (2010).
- <sup>9</sup>S. Stankovich, D. A. Dikin, G. H. B. Dommett, K. M. Kohlhaas, E. J. Zimney, E. A. Stach, R. D. Piner, S. T. Nguyen, and R. S. Ruoff, *Nature* **442**, 282 (2006).
- <sup>10</sup>J. G. Radich, R. Dwyer, and P. V. Kamat, *J. Phys. Chem. Lett.* **2**, 2453 (2011).
- <sup>11</sup>D. R. Dreyer, S. Park, C. W. Bielawski, and R. S. Ruoff, *Chem. Soc. Rev.* **39**, 228 (2010).
- <sup>12</sup>J. I. Paredes, S. Villar-Rodil, A. Martínez-Alonso, and J. M. D. Tascón, *Langmuir* **24**, 10560 (2008).
- <sup>13</sup>B. Konkana and S. Vasudevan, *J. Phys. Chem. Lett.* **3**, 867 (2012).
- <sup>14</sup>X. Li and G. B. McKenna, *ACS Macro Lett.* **1**, 388 (2012).
- <sup>15</sup>Y. Xu, W. Hong, H. Bai, C. Li, and G. Shi, *Carbon* **47**, 3538 (2009).
- <sup>16</sup>J. F. Shen, B. Yan, T. Li, Y. Long, N. Li, and M. X. Ye, *Soft Matter* **8**, 1831 (2012).
- <sup>17</sup>R. Liu, S. Liang, X. Z. Tang, D. Yan, X. Li, and Z. Z. Yu, *J. Mater. Chem.* **22**, 14160 (2012).
- <sup>18</sup>X. Zhao, Q. Zhang, D. Chen, and P. Lu, *Macromolecules* **43**, 2357 (2010).
- <sup>19</sup>T. Ramanathan, A. A. Abdala, S. Stankovich, D. A. Dikin, M. Herrera-Alonso, R. D. Piner, D. H. Adamson, H. C. Schniepp, X. Chen, R. S. Ruoff, S. T. Nguyen, I. A. Aksay, R. K. Prud'Homme, and L. C. Brinson, *Nat. Nanotechnol.* **3**, 327 (2008).
- <sup>20</sup>H. Kim, A. A. Abdala, and C. W. Macosko, *Macromolecules* **43**, 6515 (2010).
- <sup>21</sup>Y. Zhang, L. Ren, S. Wang, A. Marathe, J. Chaudhuri, and G. Li, *J. Mater. Chem.* **21**, 5386 (2011).
- <sup>22</sup>E. D. Aluker, A. G. Krechetov, B. G. Loboiko, D. R. Nurmukhametov, V. P. Filin, and E. A. Kazakova, *Russ. J. Phys. Chem. B* **2**, 375 (2008).
- <sup>23</sup>K. P. Loh, Q. L. Bao, G. Eda, and M. Chhowalla, *Nat. Chem.* **2**, 1015 (2010).
- <sup>24</sup>M. Li, X. Yang, J. Ren, K. Qu, and X. Qu, *Adv. Mater.* **24**, 1722 (2012).
- <sup>25</sup>T. Ozawa, *Bull. Chem. Soc. Jpn.* **38**, 1881 (1965).
- <sup>26</sup>T. Ozawa, *J. Therm. Anal.* **2**, 301 (1970).
- <sup>27</sup>S. Vyazovkin, A. Burnham, J. M. Criado, L. A. Perez-Maqueda, C. Popescu, and N. Sbirrazzuoli, *Thermochem. Acta* **520**, 1 (2011).
- <sup>28</sup>H. E. Kissinger, *Anal. Chem.* **29**, 1702 (1957).
- <sup>29</sup>M. Smeu, F. Zahid, W. Ji, H. Guo, M. Jaidann, and H. Abou-Rachid, *J. Phys. Chem. C* **115**, 10985 (2011).